1st LATAM-SHM 2023 Conference
A. Güemes, L. Mujica, J. Sierra (Eds)

SPATIO-TEMPORAL DAMAGE IDENTIFICATION THROUGH BAYESIAN CALIBRATION OF TIME-VARYING FINITE ELEMENT MODELS

GASTÓN PARRA*, RODRIGO ASTROZA*, MATIAS BIRREL*, FELIPE MIZÓN*

*Faculty of Engineering and Applied Sciences
Universidad de los Andes, Santiago, Chile
Monseñor Álvaro del Portillo, 12.455 Santiago, Chile
e-mail: kgparra@miuandes.cl, rastroza@miuandes.cl, mbirrel@miuandes.cl, fmizon@miuandes.cl

Key words: Damage identification, Bayesian model updating, Time varying linear system.

Abstract. Damage identification of civil structures is of primary importance following extreme events such as earthquakes. Detection, location, and quantification of damage provide crucial information to assess the state of health of a structural system. Therefore, it is imperative to develop robust and accurate methods for this purpose. In this paper, an inverse method based on Bayesian inference is proposed to calibrate time-varying finite element (FE) models representing civil structures suffering damage when subjected to seismic excitations. In the two-step approach, the time-varying modal parameters of the structure are identified using recorded input-output seismic vibration data. Then, a linear FE model is developed and calibrated at different time instants of the earthquake by updating the elastic modulus of different elements. The model calibration is conducted by minimizing the misfit between the modal properties (i.e., natural frequencies and mode shapes) using a sequential Monte Carlo inference method. To validate the effectiveness of the approach, a shake table test is carried out on a two-story scaled steel structure with elastomeric bearings at the base, which concentrate the nonlinear behavior of the structure. The results confirmed the good performance of the method in detecting, locating, and assessing the nonlinear behavior in civil structures under seismic loading.

1 INTRODUCTION

Infrastructure impacts a nation's economy, competitiveness, and society's well-being. Civil engineering structures must safeguard the lives of their occupants during operating loads and natural disasters such as earthquakes. In particular, accurate and timely identification of damage in civil structures is relevant to ensure structural safety and adequate performance after extreme events. The ability to detect, locate, and quantify damage in structures provides critical information for assessing their health condition and making decisions about the necessity of rehabilitation [1].

Model updating methods provide tools to calibrate finite element (FE) models considering observed structural response or quantities derived therefrom [2], [3]. These methods typically utilize modal properties, such as natural frequencies and mode shapes, to assess structural damage [4], [5]. The objective of finite element model updating (FEMU) is to find the optimal values of a set of parameters that best represent the experimentally measured response [6]. Probabilistic FEMU has been shown to be a robust tool for calibrating structural properties under uncertainty [7], [8].

During seismic events, structures can experience nonlinear response behavior, thus inducing variations in their modal properties due to changes in the effective stiffness and energy dissipation mechanisms [9], [10]. For this reason, using vibration data collected before and after a damage inducing event, as commonly done, seems not adequate for comprehensive damage identification. When updating linear FE models, the elastic modulus of structural components is often defined as calibration parameters. This allows to capture and quantify the impact of the effective stiffness reduction caused by localized structural damage [6]. However, it is important to track the variations of these parameter values during the seismic events since they are commonly partially recovered after the earthquake [11].

When updating numerical models, there are different sources of uncertainties that should be accounted for. Model parameter uncertainty is directly tackled in the calibration process. Modeling errors and measurement noise can be properly incorporated in some cases. Current FEMU techniques can be categorized as probabilistic and deterministic approaches. The former allows to account for uncertainties related to modeling errors and measurement noise. Bayesian methods provide a rigorous approach for probabilistic FEMU by estimating joint probability distribution of the modeling parameters being calibrated [4], [12]. Markov Chain Monte Carlo (MCMC) methods are a valuable tool employed to generate series of samples that allow to estimate posterior probability density functions (PDFs). Significant advancements have been made in the literature concerning the contributions of MCMC algorithms to Bayesian FEMU [7].

This research proposes a two-step Bayesian inference approach to calibrate FE models for civil structures subjected to seismic forces. The process begins with the identification of time-varying modal parameters of the structure using input-output seismic acceleration data. Subsequently, a linear FE model is calibrated by updating elastic modulus values at various time intervals during the earthquake. Sensitivity analysis is conducted to identify the most influential parameters on the model's responses, and model calibration is achieved using the sequential Monte Carlo inference method. A shake table experimental test is conducted on a two-story scaled steel structure with elastomeric base isolators, which exhibit nonlinear behavior during the seismic excitation, to validate the proposed approach.

2 SPATIO-TEMPORAL DAMAGE IDENTIFICATION THOUGH BAYESIAN CALIBRATION OF TIME-VARYING FINITE ELEMENT MODELS

This study introduces a methodology for spatio-temporal damage identification through Bayesian calibration of time-varying FE models. The approach is based on using time-varying dynamic properties to calibrate FE models. Dynamic properties during the earthquake are first estimated using the deterministic-stochastic subspace identification (DSI) method applied to short-time windows of input-output seismic vibration data. Then, the identified time-varying modal parameters are used to update a linear FE model using a Bayesian approach (Figure 1). A scaled structure with elastomers subjected to seismic excitation on a shaking table is presented as a case study.

An initial linear FE model, defined by the modeling parameter vector θ^{initial}, is first calibrated using the modal parameters identified from the first time-window of the earthquake data. Since a Bayesian approach is used for updating, joint posterior PDF for the updating parameters is obtained. For the following updating steps, information from the previous

updating step is used to define the prior distribution, and the likelihood function is defined based on the error between the modal parameters identified from the vibration data and their counterparts derived from the FE model. Posterior PDFs are then obtained for all the updating steps. Figure 1 summarizes the proposed approach.

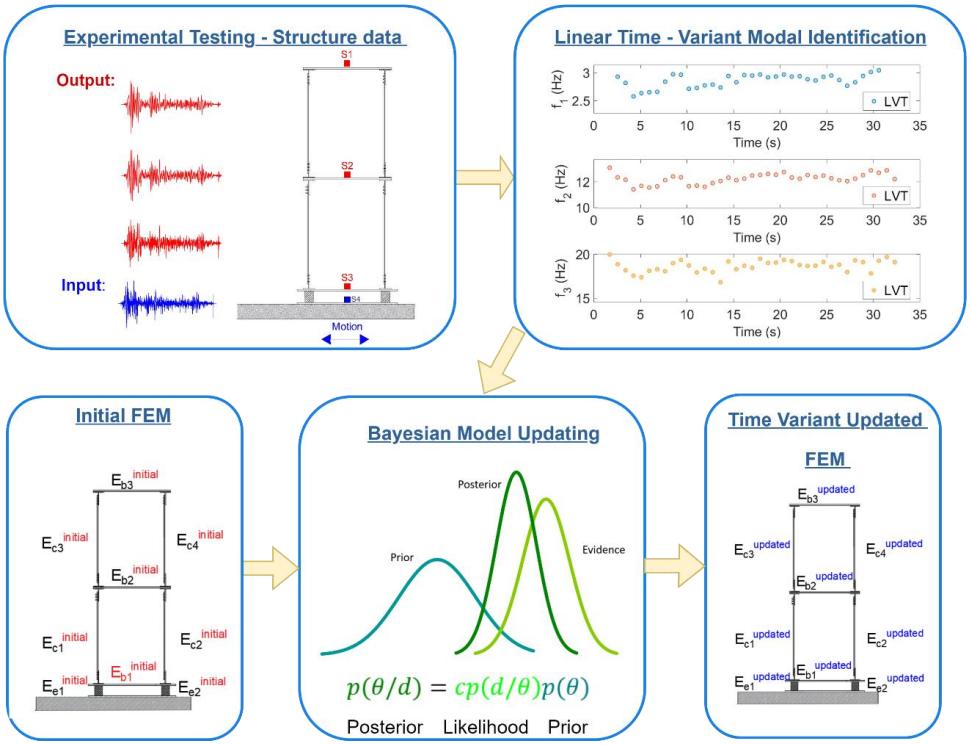

Figure 1: Proposed methodology

2.1 Linear time-variant modal identification

The DSI method [13] is employed to identify the modal parameters of the structure during an earthquake by using a short-time moving window approach [14]. The process estimates instantaneous modal properties using input-output acceleration data divided into short time windows to capture dynamic variation during the seismic event. The DSI method aims to determine system order (n) and matrices ($\mathbf{A_d}, \mathbf{B_d}, \mathbf{C_d}, \mathbf{D_d}, \mathbf{Q}, \mathbf{R}$, and $\mathbf{S}$) using s input measurements ($u_0, u_1, \dots, u_{s-1}$) and output measurements ($y_0, y_1, \dots, y_{s-1}$). Modal properties are established by obtaining the eigenvalues and eigenvectors of matrices $\mathbf{A_d}$ and $\mathbf{C_d}$ as expressed below:

$$f_r = \frac{\sqrt{\lambda_r \lambda_r^*}}{2\pi} \quad r=1, \dots, n/2 \tag{1}$$

$$\xi_r = \frac{-Re(\lambda_r)}{|\lambda_r|} \quad r=1, \dots, n/2 \tag{2}$$

$$\phi_r = \mathbf{C_d}\Psi = [\phi_1, \dots, \phi_{n/2}\ ] \tag{3}$$

Where f_r represents the modal frequencies, ξ_r and ϕ_r denote the modal damping ratio and mode shape, respectively, λ_r are the eigenvalues of the continuous-time state matrix $\mathbf{A_c}$ (with $\mathbf{A_d} = e^{\mathbf{A_c}\,\Delta t}$), Ψ refers to the eigenvectors of $\mathbf{A_c}$.

The minimum window length (s_{min}) defined in Eq. (4) with 50% overlapping is used for linear-time varying system identification based on seismic input-output data [14]. In Eq. 4, m is the number of inputs, l is the number of outputs, and i is the number of block rows of the Hankel matrices. Stabilization diagrams are utilized to differentiate between physical and spurious modes within each short-window data set [15].

$$s_{min} = 2i(m + l + 1) \tag{4}$$

2.2 Description of test structure and instrumentation

The case study is a two-story steel structure with elastomeric supports at the base. The structure has one bay in each direction, with plan dimensions of 0.30 m in longitudinal and transversal directions. The height of the columns was 0.34 m (see Figure 2b), and the elastomers had a height of 0.04 m. The total weight of the structure was approximately 0.135 kN. The floor system consisted of 5 mm thick steel plates at each level. Every story is supported by four columns with a cross-section of 0.03m×0.003m, connected to a steel joint. Elastomers with cross-section of 0.03m×0.03m were positioned at the base of the specimen. Instrumentation for the test consisted of three accelerometers placed at the center of each floor and one at the base, as depicted as Figure 2b. The accelerometer model used was Endevco 44A16 with a full-scale range of ±50 g. The data acquisition system (DAQ) was a Quantum CX22-B from HBM. The data was sampled at 300 Hz.

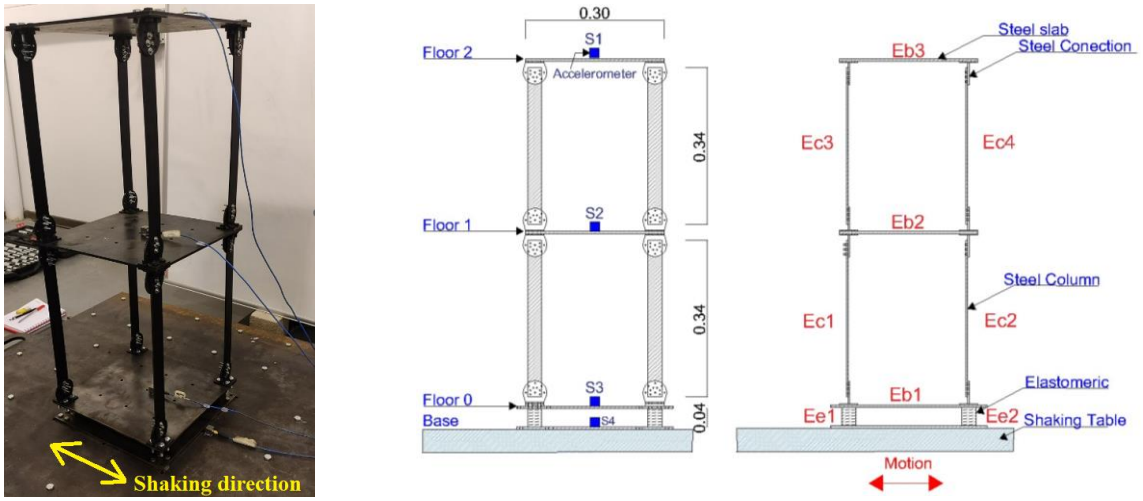

Figure 2: Test structure: (a) General view of the structure; (b) front view (units: m); (c) lateral view of the model

2.3 Global sensitivity analysis

Global sensitivity analysis (GSA) simplifies the selection of the most influential parameters for creating a validated surrogate model that effectively captures the system's variability without requiring all the original parameters. The analysis helps to understand how "input" parameters introduce variations in "output" results and assesses interactions among parameters when determining their impact on the model's response. GSA provides indices to measure effects of individual parameters and also interacting effects between different model parameters. A calculation of Sobol's indices based on Polynomial Chaos Expansion (PCE) [16] was performed using MATLAB library UQlab. The GSA model uses nine parameters, a

confidence level of 99%, and a tolerance level of 10% of the Monte Carlo error of the variability distribution. To achieve this objective, the model is executed 3000 times, and a surrogate third order PCE model is constructed to capture the model responses.

2.4 Bayesian finite element model updating

In the context of probabilistic model updating, the Bayesian approach effectively integrates prior beliefs and observed data to reduce parameter uncertainty. The Bayes theorem (Eq. 5) is employed to calculate the posterior probability distribution, denoted as $p(\boldsymbol{\theta}|\mathbf{d})$, which represents the updated parameters ($\boldsymbol{\theta}$) based on recorded data or information derived therefrom ($\mathbf{d}$). The normalization constant (c), called evidence, ensures that the posterior PDF integrates to one. Additionally, the likelihood function $p(\mathbf{d}|\boldsymbol{\theta})$ quantifies the probability of observing the recorded data ($\mathbf{d}$) given the parameters ($\boldsymbol{\theta}$), essentially assessing how well the model, with the current parameter values, explains the observed data. Lastly, the prior PDF $p(\boldsymbol{\theta})$ reflects the initial understanding of the updating parameters.

$$p(\boldsymbol{\theta}|\mathbf{d}) = cp(\mathbf{d}|\boldsymbol{\theta})p(\boldsymbol{\theta}) \tag{5}$$

In this study, prior PDFs are modeled as lognormal distributions, assuming mutually independent parameters. Model calibration minimizes the discrepancy between model-predicted and experimental dynamic properties by estimating an optimal configuration of model parameters using an error function under the assumption of zero-mean Gaussian distributions.

$$e_{\lambda i} = \frac{\tilde{\lambda}_i - \lambda(\boldsymbol{\theta})}{\tilde{\lambda}_i} \tag{6}$$

$$\boldsymbol{e}_{\boldsymbol{\Phi} i} = \frac{\widetilde{\boldsymbol{\Phi}}_i}{\|\widetilde{\boldsymbol{\Phi}}_i\|} - a_i \frac{\boldsymbol{\Gamma}\boldsymbol{\Phi}_i(\boldsymbol{\theta})}{\|\boldsymbol{\Gamma}\boldsymbol{\Phi}_i(\boldsymbol{\theta})\|} \tag{7}$$

Where $e_{\lambda i}$ is the eigenfrequency error; $\tilde{\lambda}_i = (2\pi\tilde{f}_i)^2$ is the square of the experimental natural frequency; $\lambda(\boldsymbol{\theta})$ is the squared natural frequency of the model considering the parameters $\boldsymbol{\theta}$; $\boldsymbol{e}_{\boldsymbol{\Phi} i}$ is the mode shape error; $\widetilde{\boldsymbol{\Phi}}_i$ is the mode shape vector of the i^{th} mode extracted experimentally; and $\boldsymbol{\Phi}_i(\boldsymbol{\theta})$ is the mode shape vector of the model considering the parameters $\boldsymbol{\theta}$ of the i^{th} mode. Finally, $\boldsymbol{\Gamma}$ serves as a mapping matrix that establishes a correspondence between the model modal coordinates and the sensor positions used to extract modal properties from experimental data, and a_i is defined as follow:

$$a_i = \frac{\widetilde{\boldsymbol{\Phi}}_i \, \boldsymbol{\Gamma} \, \boldsymbol{\Phi}_i(\boldsymbol{\theta})}{\|\widetilde{\boldsymbol{\Phi}}_i\| \, \|\boldsymbol{\Gamma}\boldsymbol{\Phi}_i(\boldsymbol{\theta})\|} \tag{8}$$

The posterior PDF based on the selected likelihood function (error functions) and prior PDF, can be formulated as shown below:

$$p(\boldsymbol{\theta}|\mathbf{d}) \propto exp\left(-\frac{1}{2}J(\boldsymbol{\theta}, \mathbf{d})\right) \tag{9}$$

where $J(\boldsymbol{\theta},\mathbf{d})$ is:

$$J(\boldsymbol{\theta}, \mathbf{d}) = \sum_{i=1}^{m} \frac{(e_{\lambda_i})^2}{\sigma_{\lambda_i}^2} + \sum_{i=1}^{m} \frac{\boldsymbol{e}_{\boldsymbol{\Phi}_i}^T \cdot \boldsymbol{e}_{\boldsymbol{\Phi}_i}}{\sigma_{\Phi_i}^2} \tag{10}$$

Where, m denotes the number of modes considered, σ_{λ_i} is the standard deviation of the i^{th} frequency and σ_{Φ_i} is the standard deviation of the shape modes component for the i^{th} mode. The joint posterior distribution is estimated using the simulation method of MCMC, which is a numerical approach for estimating the posterior distribution of updating parameters.

3 RESULTS

3.1 System identification results and earthquake excitation

The north-south component of the "El Centro" motion, that occurred on May 18, 1940, with a magnitude (Mw) of 6.9, served as the input for the test. To perform the DSI, acceleration records in the direction of excitation are used. The input signal is defined as the acceleration applied by the shaking table and the output signals are the three signals recorded on upper floors. The number of rows of the Hankel matrices *(i)* is selected equal to 50 and meet the procedure presented in [18]. According to Eq. 4, $s_{mín}$ is (2×50(1+3+1)) = 500, and the sampling frequency is 300 Hz. Then, the minimum window length is equal to (500/300) = 1.70 s. A 50% overlap is used for all windows, except the first one, resulting in the estimation of instantaneous modal parameters every 0.85 s. The "instantaneous" natural frequencies of the first three longitudinal modes and the recorded time history of input acceleration from the shake table are presented in Figure 3. As the amplitude of the input motion increases during the strong-motion phase, the system's frequencies decrease significantly. However, by the end of the test, the frequencies recover, returning to values similar to those identified at the beginning of the test. The frequencies of the structure at the beginning of the test are: f_1=3.48 Hz for the first mode, f_2=13.11 Hz for the second mode, and f_3=19.98 Hz for the third mode. The maximum reduction in frequency during the test are 35.41%, 14.71%, and 13.80% for the first, second, and third modes, respectively.

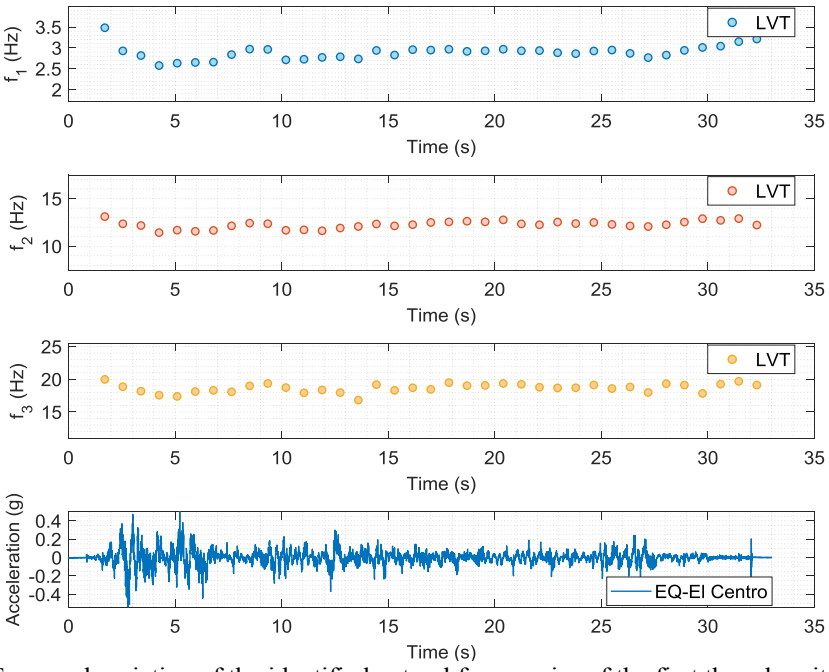

Figure 3: Temporal variation of the identified natural frequencies of the first three longitudinal modes

3.2 Linear FE model and sensitivity analysis

A 2D linear FE model is employed, with three degrees of freedom at each node. The masses are lumped at the nodes. The elastomeric bearing elastic modulus is referred as E_{ei}, while the Young´s modulus of steel columns and steel slabs are denoted as E_{ci} and E_{bi}, respectively. The slabs are modeled as beams with a width equal to half the plate width. Each component in the linear FE model is discretized into five elements. The FE model is illustrated in the Figure 2c.

GSA is conducted on the linear FE model to identify the most influential parameters in the modal parameters. The elasticity modulus of the nine elements of the structures was sampled, employing a lognormal distribution with a mean of 1.17 MPa with a standard deviation of 0.30 MPa for the elastomers, while for elements of structural steel, the mean of the lognormal distribution is set to 200 GPa and the standard deviation to 20 GPa. The total Sobol indices S_T obtained for each parameter for the first three natural frequencies and mode shapes are presented in Figure 4. The parameter of the elastomeric elements (Ee) are the most influential in the model's variability for all three frequencies modes, obtaining S_T values close to 0.50; 0.32; and 0.50. On the other hand, slabs parameters (E_{b1}, E_{b2}, and E_{b3}) have minor influence on the natural frequencies of the model. Finally, for the next steps, the following five out of the nine parameters were selected for estimation: E_{e1}=E_{e2}, E_{c1}, E_{c2}, E_{c3}, and E_{c4}. The values of $Ee1$ and $Ee2$ are assumed equals to reduce computational time and because the same material was used for both bearings.

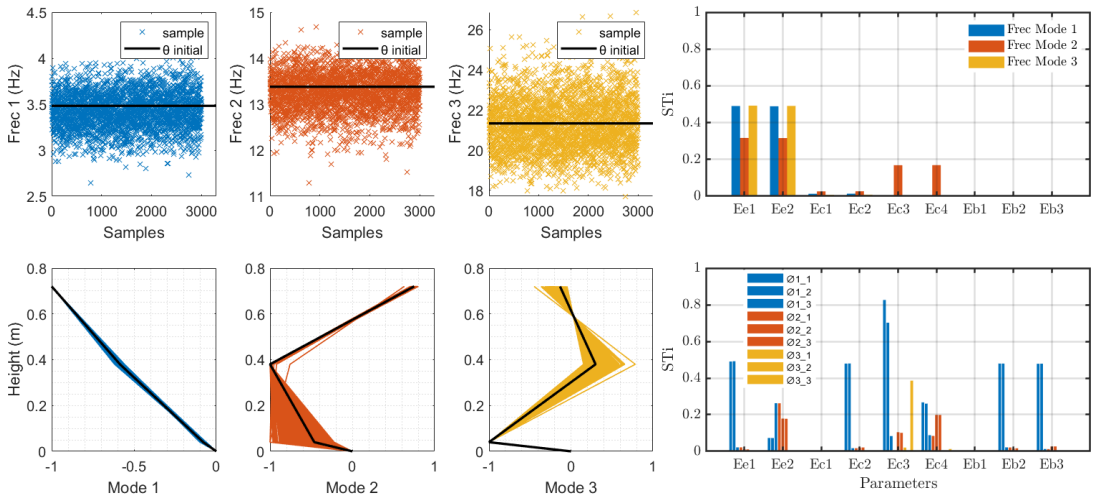

Figure 4: Total Sobol's indices for the first three frequencies and mode shapes of the linear FE model

3.3 Model Updating Results

The elastomeric and steel material's modulus of elasticity of the five specifically chosen components of the linear FE model are used as parameters to be calibrated. For model updating, these parameters are normalized as the ratio between the updated elasticity modulus and the corresponding initial value:

$$\theta_i = \frac{E_i^{updated}}{E_i^{initial}} \quad \text{with } i = 1, \dots, 5 \tag{11}$$

Model calibration is conducted every 0.85 s according to the DSI results. The prior PDFs are considered as lognormal distributions, mean values of $E_i^{initial}$ were taken equal to 1.17 MPa for elastomeric and 200 GPa for the steel material. The standard deviation of updating parameters is set at 25% for elastomeric material and 10% for steel. MCMC simulation method is employed with a total of 2200 samples and 4 chains, which meets the requirements outlined in [17]. The initial calibration results for the first updating step are as follows: 1.04 MPa for elastomeric, 198.80 GPa for both columns of the first floor, and 202.40 and 202.20 GPa for the columns of the second floor. The evolution of the marginal posterior PDF at the beginning of the test is presented in Figure 5, for the first three processed time windows (1.70, 2.55, 3.40 s). In this figure, one element from each floor is represented, i.e., E_{e1}, E_{c1}, and E_{ec3}.

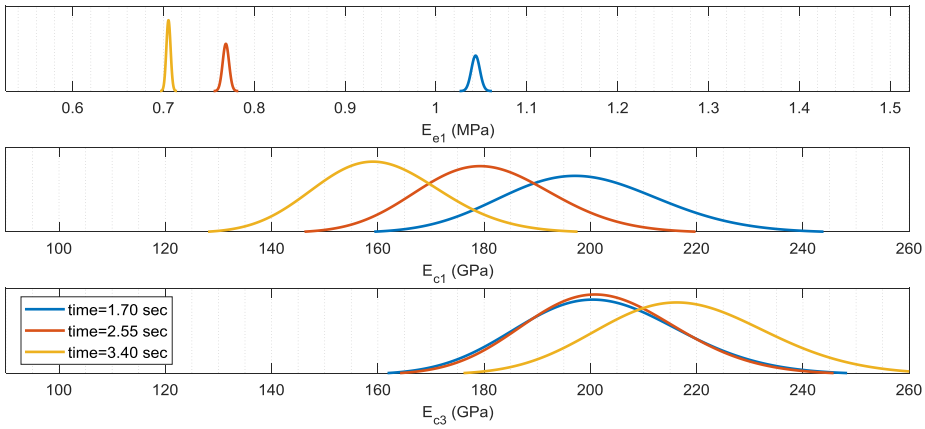

Figure 5: Evolution of the marginal posterior PDF for the time 1.70 to 3.40 s.

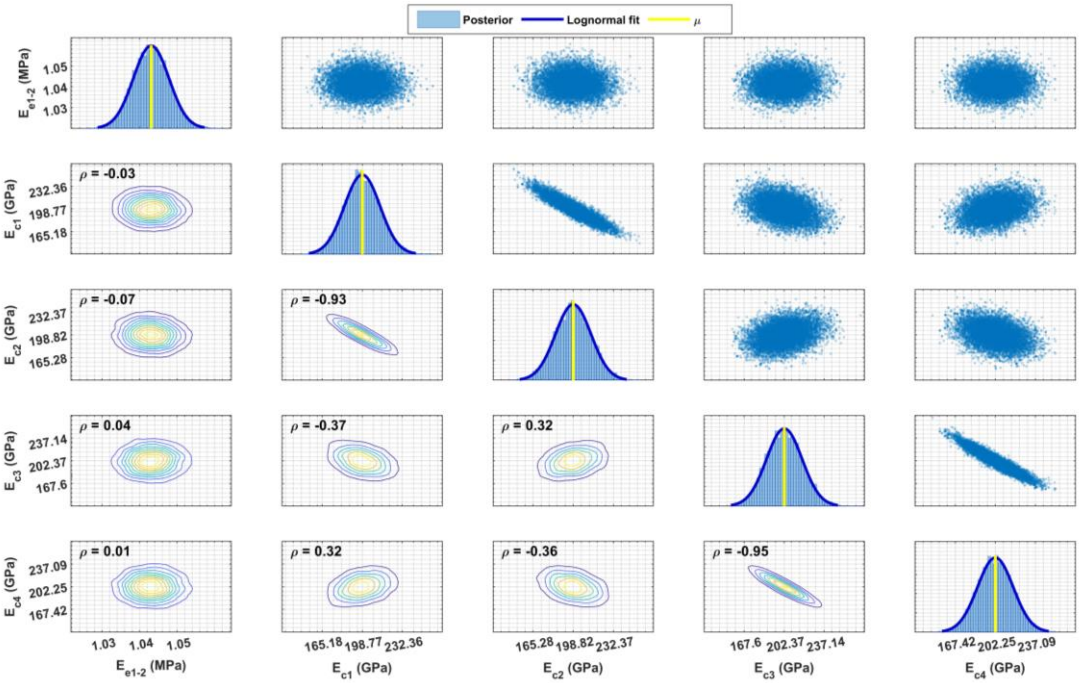

Figure 6: Sample of parameter posteriors estimation result at *t*=1.70 s.

In Figure 6, the sample posteriors (marginal and bivariate) at updating time t=1.7 s are presented. At the upper diagonal, scatter plots of pairs of variables' distributions are displayed, where darker regions indicate a higher concentration of samples. Along the diagonal, histograms of the marginal posteriors are shown, also a log-normal distribution fit is presented. Additionally, the mean values are highlighted in yellow. Below the diagonal, contour plots and Pearson's correlation coefficients (ρ) are illustrating the degree of linear correlation between each pair of parameters. Strong correlations are found among columns on the same floor, with coefficients of -0.95 for first-floor columns and -0.98 for second floor columns. No other significant correlations are observed between modeling parameters.

The variations of the elastic modulus of the elements along the seismic excitation are presented in Figure 7. It is noted that the modulus of elasticity $E_{e1\text{-}2}$ in the elastomeric material undergoes significant changes due to its nonlinear behavior during the test. Conversely, the steel columns exhibit lower variations in their elastic modulus values that remain close to the initial value, potentially attributed to the flexibility of the connections. These changes are influenced by the increment of the amplitude of the input acceleration. As the accelerations decrease towards the end of the seismic test, the elastic modulus tends to recover, approaching their initial values. This pattern suggests a close correlation between earthquake intensity and the changes in modal parameters. The 5th and 95th percentile limits are presented alongside the mean values, where very low estimation uncertainty is observed in the elastic modulus of elastomeric bearings.

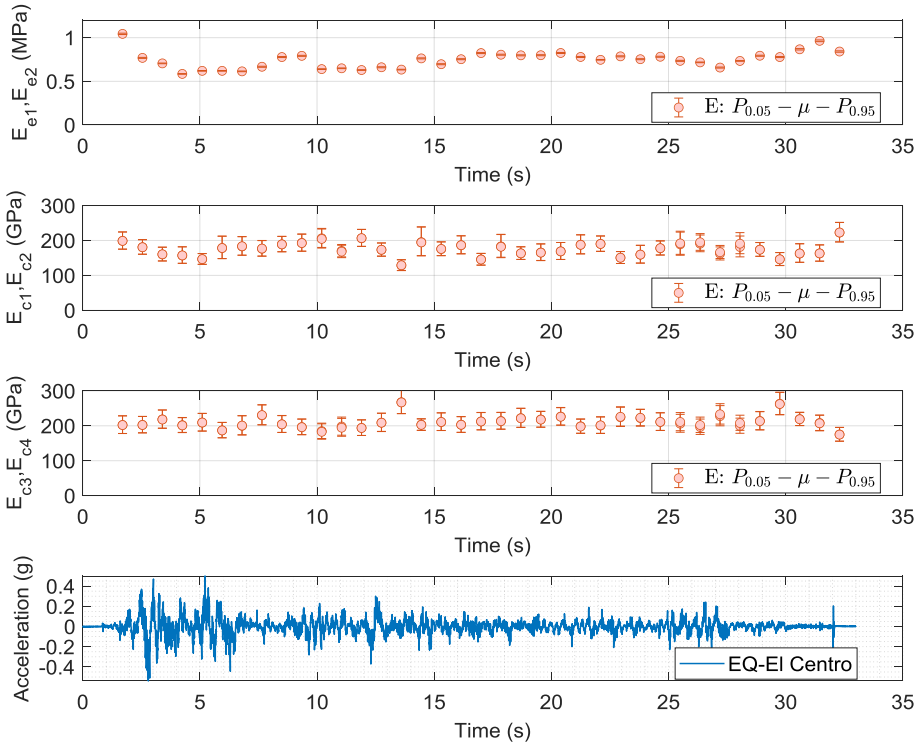

Figure 7: Variation of the parameters during the shaking table test

To analyze the effect of propagating the parameter estimation uncertainties in the modal parameters of the model, 1000 responses were simulated at each step time using the posterior

PDFs of the parameters $\boldsymbol{\theta}^{updated}$. This was performed to compare the natural frequencies and mode shapes of the model against the experimental data. Figure 8 shows identified natural frequencies with their model-predicted counterparts ($\mu^{estimated}$) computed based on updated parameters ($\boldsymbol{\theta}^{updated}$) at each updating time step. Additionally, the 5th and 95th percentiles are presented. The results obtained for $\mu^{estimated}$ are used to compare the updated natural frequencies of the model with the experimentally identified. The average global error for all the updating steps is 1.98%, 0.33%, and 2.19% for the first, second, and third natural frequencies, respectively. The Modal Assurance Criterion (MAC) is employed to compare the identified and model mode shapes. The estimated mode shapes are considered as the mean of the thousand samples generated from the updated linear FE model. The MAC values are very close to 1.0, suggesting that the mode shapes predicted by the linear FE model are consistent with their identified counterparts.

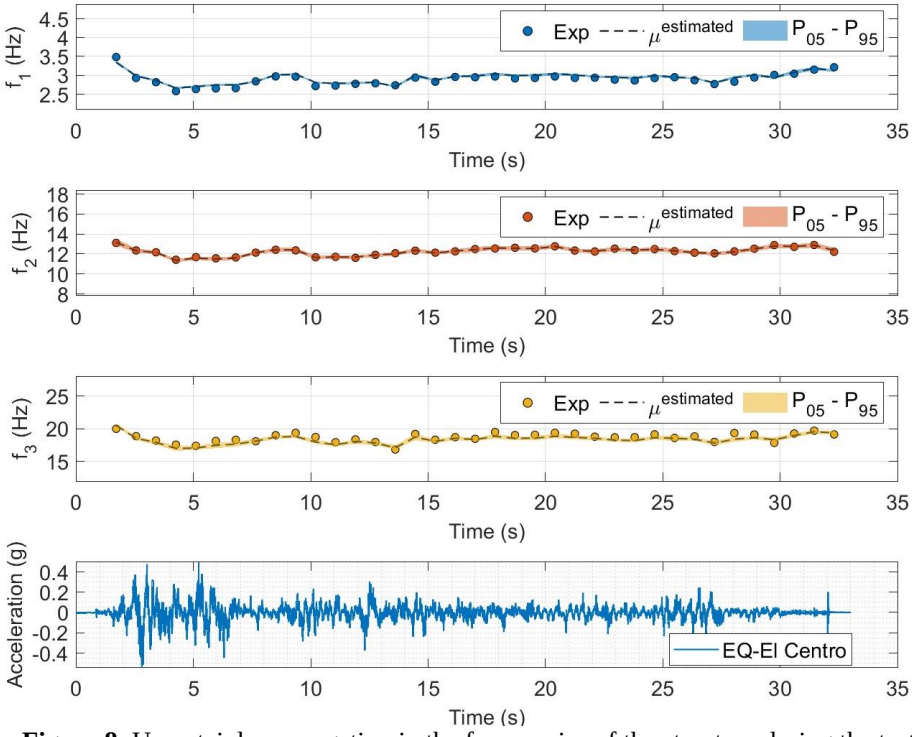

Figure 8: Uncertainly propagation in the frequencies of the structure during the test

4 CONCLUSIONS

The Bayesian calibration of time-varying FEM for spatio-temporal damage identification is a robust method for assessing structural integrity during seismic events. It employs short-time windows of dynamic data for FEM updates, facilitating damage detection and localization. Global sensitivity analysis identifies influential parameters, focusing on those impacting the model's response. Bayesian calibration with lognormal prior PDFs assesses uncertainties and identifies nonlinear behavior locations. This methodology effectively captures dynamic property changes during seismic events, including frequency and mode shape variations. It successfully identifies the first three frequencies and vibration modes using short time

windowing. Bayesian updates align responses closely with experimental data. Non-linear behavior in elastomers was consistently detected throughout the test, indicating potential for real-time structural health monitoring. Average global errors were 1.98% for the first frequency, 0.33% for the second, and 2.19% for the third. Mode shape comparisons using MAC showed consistent results between experimental and predicted mode shapes.

ACKNOWLEDGMENTS

This research was funded by the Chilean National Research and Development Agency (ANID) through the FONDECYT project 1200277. G. Parra acknowledges the financial support from ANID grant Doctorado Nacional #21220870.

REFERENCES

[1] E. Asadi, A. M. Salman, Y. Li, and X. Yu, "Localized health monitoring for seismic resilience quantification and safety evaluation of smart structures," *Structural Safety*, vol. 93, Nov. 2021, doi: 10.1016/j.strusafe.2021.102127.

[2] J. E. Friswell M. I. and Mottershead, "Finite Element Modelling," in *Finite Element Model Updating in Structural Dynamics*, Dordrecht: Springer Netherlands, 1995, pp. 7–35. doi: 10.1007/978-94-015-8508-8_2.

[3] B. Jaishi and W. Ren, "Structural Finite Element Model Updating Using Ambient Vibration Test Results," no. July, 2019, doi: 10.1061/ASCE0733-94452005131.

[4] S. Ereiz, I. Duvnjak, and J. Fernando Jiménez-Alonso, "Review of finite element model updating methods for structural applications," *Structures*, vol. 41. Elsevier Ltd, pp. 684–723, Jul. 01, 2022. doi: 10.1016/j.istruc.2022.05.041.

[5] A. Nozari, I. Behmanesh, S. Yousefianmoghadam, B. Moaveni, and A. Stavridis, "Effects of variability in ambient vibration data on model updating and damage identification of a 10-story building," *Eng Struct*, vol. 151, pp. 540–553, Nov. 2017, doi: 10.1016/j.engstruct.2017.08.044.

[6] F. Mizon, M. Birrell, J. Abell, and R. Astroza, "Probabilistic Time-Variant Linear Finite Element Model Updating for Nonlinear Structural Systems," in *Experimental Vibration Analysis for Civil Engineering Structures*, T. and D. J. and A. R. Wu Zhishen and Nagayama, Ed., Cham: Springer International Publishing, 2023, pp. 349–363.

[7] J. Mao, H. Wang, and J. Li, "Bayesian Finite Element Model Updating of a Long-Span Suspension Bridge Utilizing Hybrid Monte Carlo Simulation and Kriging Predictor," *KSCE Journal of Civil Engineering*, vol. 24, no. 2, pp. 569–579, Feb. 2020, doi: 10.1007/s12205-020-0983-4.

[8] J. Wu, Q. Yan, S. Huang, C. Zou, J. Zhong, and W. Wang, "Finite Element Model Updating in Bridge Structures Using Kriging Model and Latin Hypercube Sampling Method," *Advances in Civil Engineering*, vol. 2018, 2018, doi: 10.1155/2018/8980756.

[9] K. Zhou and Q. Li, "Effects of time-variant modal frequencies of high-rise buildings on damping estimation," *Earthq Eng Struct Dyn*, vol. 50, no. 2, pp. 394–414, Feb. 2021, doi: 10.1002/eqe.3336.

[10] B. Moaveni and E. Asgarieh, "Deterministic-stochastic subspace identification method for identification of nonlinear structures as time-varying linear systems," *Mech Syst Signal Process*, vol. 31, pp. 40–55, 2012, doi: 10.1016/j.ymssp.2012.03.004.

[11] A. Astorga and P. Guéguen, "Structural health building response induced by earthquakes: Material softening and recovery," *Engineering Reports*, vol. 2, no. 9, pp. 1–9, 2020, doi: 10.1002/eng2.12228.
[12] S. Mustafa, N. Debnath, and A. Dutta, "Bayesian probabilistic approach for model updating and damage detection for a large truss bridge," *International Journal of Steel Structures*, vol. 15, no. 2, pp. 473–485, Jun. 2015, doi: 10.1007/s13296-015-6016-3.
[13] P. Van Overschee and B. De Moor, "Subspace Identification for Linear Systems," *Conference Proceedings of the International Conference of IEEE Engineering in Medicine and Biology Society*, vol. 2008, no. 6, pp. 4427–30, 2008, doi: 10.1109/IEMBS.2008.4650193.
[14] R. Astroza, G. Gutiérrez, C. Repenning, and F. Hernández, "Time-variant modal parameters and response behavior of a base-isolated building tested on a shake table," *Earthquake Spectra*, vol. 34, no. 1, pp. 121–143, 2018, doi: 10.1193/032817EQS054M.
[15] B. Peeters and G. De Roeck, "One-year monitoring of the Z24-bridge: Environmental effects versus damage events," *Earthq Eng Struct Dyn*, vol. 30, no. 2, pp. 149–171, 2001, doi: 10.1002/1096-9845(200102)30:2<149::AID-EQE1>3.0.CO;2-Z.
[16] I. M. Sobol′, "Global sensitivity indices for nonlinear mathematical models and their Monte Carlo estimates," *Math Comput Simul*, vol. 55, no. 1–3, pp. 271–280, Feb. 2001, doi: 10.1016/S0378-4754(00)00270-6.
[17] D. Vats, J. M. Flegal, and G. L. Jones, "Multivariate output analysis for Markov chain Monte Carlo," *Biometrika*, vol. 106, no. 2, pp. 321–337, Jun. 2019, doi: 10.1093/biomet/asz002.
[18] C. Rainieri and G. Fabbrocino, "Influence of model order and number of block rows on accuracy and precision of modal parameter estimates in stochastic subspace identification," *International Journal of Lifecycle Performance Engineering*, vol. 1, no. 4, p. 317, 2014, doi: 10.1504/ijlcpe.2014.064099.